SO_x Storage Materials under Lean−Rich Cycling Conditions—Part II: Influence of Pt, H_2O, and Cycling Time

Hendrik Dathe, Peter Haider, Andreas Jentys, and Johannes A. Lercher*

Technische Universität München, Department of Chemistry, Lichtenbergstrasse 4, D-85747 Garching, Germany

Received: July 12, 2006; In Final Form: October 20, 2006

The role of Pt and the influence of the reaction conditions during lean−rich cycling experiments were studied on a second generation SO_x trapping material. The combination of the Generalized 2-D Correlation Analysis, 2-D Sample−Sample Correlation Analysis, and Factor Analysis using the MCR-ALS technique was applied to identify the reactive species. Transient surface sulfate species were formed under oxidative reaction conditions (lean mode) and decomposed under reducing reaction conditions (rich operation mode). The reduction of this species was identified to be the main contribution to the SO_2 release observed under dynamic flow conditions. Pt facilitates the formation of sulfates but also catalyzes the reduction of the transient surface sulfate species leading to a higher amount of SO_2 released under rich conditions. In the presence of water, this effect was diminished, which was found to be mainly a result of the suppressed formation of surface sulfate species caused by the faster transport of SO_2 into the bulk phase of the SO_x trapping component ($BaCO_3$). Increasing the time under reducing conditions in the cycles leads to an enhanced reduction of the surface during rich conditions. The presence of water did not influence the bulk type species. It is proposed that for effective SO_2 storage materials, strong SO_x adsorption sites on the surface, the presence of water, and a short time under reducing conditions are essential.

Introduction

Lean burn engines offer significant advantages with respect to the gasoline efficiency and emission of the greenhouse gas CO_2 as compared to Otto engines (operating at stoichiometric fuel/air ratios). Nevertheless, for meeting EURO IV criteria, new techniques for emission control are necessary, especially for the reduction of the NO_x emissions. The implementation of the Nitrogen Storage-Reduction concept (NSR), which is based on a cyclic engine operation mode, is mainly limited by the presence of sulfur in the exhaust gas stream due to the formation of a thermodynamically favored sulfate species leading to the blockage of NO_x sorption sites.[1−3] A promising approach to overcome this limitation is the implementation of a SO_x trap to remove the sulfur species present in the exhaust gas stream before reaching the NSR catalyst. An important parameter of S trapping material, the fast oxidation of SO_2 to SO_3 is typically realized by adding Pt as an oxidation component. Recent publications indicate that first row transition metals (Mn and Cu) also offer a sufficient oxidation capacity and could, therefore, be used instead of Pt.[4,5] Alkaline or rare earth metals (Ca, Ba, and Mg) are usually used for the irreversible adsorption of SO_3 under oxidizing conditions.[6,7] Apart from a high sulfur storage capacity, an essential feature of S trap materials is the stability of the sulfur species under reducing (fuel rich) reaction conditions to avoid the release of SO_x during the periodic regeneration cycles of the NSR catalyst.[8,9]

The investigations performed under reducing conditions mainly addressed the regeneration potential of the trapping components and suggested that only partial regeneration is possible at high temperatures.[7,10] Nevertheless, a similar study on a second generation SO_x trap indicated even the reduction of a sulfate/sulfite type species under real cycling operation conditions at low temperatures causing SO_2 release under these conditions.[11] In part one of this publication, we investigated the stability of the sulfate species under reducing and oxidizing conditions and showed that the combination of advanced chemometric techniques and in situ IR spectroscopy allows the unequivocal identification of transient surface sulfate species formed under lean−rich conditions, which can be reduced and contribute to SO_2 in the exhaust gas stream.[12]

In part two, we address the effect of the time under reducing conditions, the presence of water, and the influence of Pt on the formation of the transient sulfur species on a second generation SO_x trapping material. Plug flow reactor experiments in combination with the results obtained from time-resolved in situ IR spectroscopy at typical diesel exhaust gas conditions will lead to an identification of the key parameters for the dynamic storage of sulfur on advanced trap materials.

Experimental Procedures

Materials. A $CuO-Al_2O_3$ mixed oxide was synthesized by a proprietary sol−gel procedure of Venezia Tecnologia and calcined in air at 823 K for 3 h. The support was further impregnated with Ba^{2+} (10%) and calcined again in air at 823 K for 1 h. Finally, the material was impregnated with Pt (1%) followed by a recalcination at 823 K for 1 h. The catalysts are denoted as $Ba/CuO-Al_2O_3$ for the Pt free sample and $Ba/CuO-Al_2O_3$ Pt for the sample impregnated with Pt.

In Situ IR Experiments. IR experiments were carried out in a flow cell in transmission mode with a Perkin-Elmer 2000−FTIR spectrometer. For the IR measurements, the samples were pressed into self-supporting wafers. The gas composition of the mixture under lean and rich conditions is shown in Table 1. All experiments were carried out at 523 K. The cycling times

* Corresponding author. Fax: +49 89 289 13544; tel.:+49 89 289 13540; e-mail: johannes.lercher@ch.tum.de.

10.1021/jp064387p CCC: $33.50
Published on Web 11/30/2006

TABLE 1: Gas Compositions Applied during in Situ IR and SO_x Uptake Experiments

gas	lean operation	rich operation
SO_2	10 ppm	10 ppm
O_2	12%	4%
CO_2	4%	8.5%
SO_2	10 ppm	10 ppm
NO_2	30 ppm	50 ppm
C_3H_6	0%	0.5%
H_2	0%	1%
He	balance to 200 mL/min	balance to 200 mL/min

were typically set to 240 s for lean operation mode and 18 s for rich operation mode. Prior to the lean−rich cycling operation, a 2 h treatment under lean conditions was performed.

SO_2 Uptake Experiments. The SO_x uptake experiments were performed at the same temperature under dynamic conditions using a tubular reactor system already described in ref 4. Typically, 50 mg of the sample with a particle size of 0.1−0.3 mm and 100 mg of SiC ($d > 0.6$ mm) were mixed and exposed to the reactant gas mixture in a quartz tube with a 4 mm inner diameter. The same gas mixtures were used for the in situ IR experiments and the SO_2 uptake experiments. The SO_2 concentration in the exhaust gas stream was determined using an SO_2 analyzer (Thermo Environmental Instruments, Model 43C). The cycling times were typically set to 240 s for lean operation mode and various times for rich operation mode.

Mathematical Methods. A detailed description of the mathematical background was included in part one.[12] Briefly, the calculation of the synchronous correlation plot was performed applying the matrix multiplication approach[13] as shown in eq 1.

$$\Phi(\nu_1, \nu_2) = \frac{1}{n-1} DD^{\mathrm{T}}$$

The data matrix D presents the mean centered spectra. The synchronous 2-D correlation intensity $\Phi(\nu_1, \nu_2)$ is regarded as the covariance between the intensities at the spectral frequencies ν_1 and ν_2 of the two series of spectra measured as function of time. Auto correlation peaks located on the diagonal line corresponding to $\nu_1 = \nu_2$ for $\Phi(\nu_1, \nu_2)$ are always positive (note that this is not necessarily true for heterospectral analysis, i.e., when two independent datasets are correlated) and form a square with two symmetric cross-peaks at the corresponding intersections. The sign of the cross-peaks indicates whether the changes are directly or reversibly (indirectly) correlated, that is, if the changes in intensity occur in the same (positive sign) or in different directions (negative sign).

The 2-D Sample−Sample Correlation Analysis was performed applying eq 2. With this technique, a detailed investigation of the periodical behavior of the spectral intensities of interest was performed following the concentration profiles directly. The cross-product matrix $F_1(n_1, \nu_2)$ represents the correlations between the different spectra of the dataset D, while the wavenumber−wavenumber 2-D Correlation Analysis Φ-(ν_1, ν_2) shows the relation among the spectral variables (e.g., wavenumbers).[14]

$$\Phi_1(\nu_1, \nu_2) = \frac{1}{n-1} D^{\mathrm{T}} D$$

−The number of principle components was selected using the approach described by Malinowski[15] and Tauler et al.[16] Prior to the calculations, the background correction was performed using the concept by Mazet et al.[17] A moving window approach involving five consecutive spectra was used as data set; hence, the data set covers either spectra recorded under lean mode or spectra recorded under lean and rich operation mode. All calculations were performed using Matlab 6.5.

Results

Properties of the Materials. Only CuO, γ-Al_2O_3, and $BaCO_3$ were identified by XRD indicating the presence of $BaCO_3$ agglomerates on the CuO−Al_2O_3 support. N_2 physisorption on the Pt free sample resulted in a BET surface area of 176 m^2/g with a sharp peak in the pore size distribution at 60 Å. The impregnation with Pt did not affect the physicochemical properties of the support. Temperature programmed desorption led to a release of 9.46 μmol of CO_2/g, which is equal to 9.8 wt % of Ba on the Pt free sample and in perfect agreement with the amount of Ba^{2+} used for the impregnation.

SO_2 Uptake Experiments. Figure 1 shows the plug flow experiments carried out under lean−rich cycling conditions in the absence of water on the Ba/CuO−Al_2O_3 material (A) and the Pt containing material (B) at 144 s of reducing conditions. Further experiments performed under different times of reducing conditions (18, 36, and 72 s) showed a similar trend. The time of oxidizing conditions was kept constant at $t = 240$ s. The inset in Figure 1 shows a magnification of the first 200 min time-on-stream. The lower SO_2 content in the exhaust gas stream under oxidizing conditions (lean) as compared to the reducing conditions (rich) indicates the almost complete SO_2 removal during the first 60 min time-on-stream. However, switching to rich operation conditions led to an increase in the concentration of SO_2 in the exhaust gas stream resulting from a release and/or decomposition of the sulfur species present on the sample. The constant SO_2 content in the exhaust gas under cycling conditions on the Pt free sample at 1000 min (Figure 1A) revealed the complete saturation of the material. It is clearly seen that with increasing numbers of cycles, the height of the desorption peaks increases while applying fuel rich conditions, indicating an increasing amount of SO_2, released under these conditions as compared to the fresh material. Figure 1B shows the lean−rich cycling experiments carried out on the Pt containing sample. In comparison to the Pt free sample, a constant SO_2 level in the exhaust gas stream was not reached even after 1000 min. Under oxidizing conditions, SO_2 was completely removed from the exhaust gas stream, while switching to reducing conditions led to a release of SO_2 (indicated by a higher intensity of the SO_2 detected). The increase of the total number of cycles was accompanied by an enlarged release of SO_2 under fuel rich conditions. Furthermore, during time-on-stream, a constant SO_2 release under these conditions was not reached as shown in Figure 1B. Figure 2 depicts the average SO_2 amount released per cycle with the dependence of the reduction time for the Pt free and Pt containing sample between the first 50 min (A) and between 950 and 1000 min time-on-stream. With both samples investigated, the amount of SO_2 released increased with increasing the time of reducing conditions. At short time-on-stream, the Pt free material released a lower amount as compared to the Pt containing material. This effect was inverse with increasing time-on-stream (see Figure 2B).

Influence of Water. Figure 3 shows the lean−rich cycling experiment carried out with 72 s reducing time in presence of 10% water added to the gas composition summarized in Table 1. The SO_2 storage was similar to that observed under dry conditions (see Figure 1). The complete adsorption of SO_2 was only observed during the first 100 min time-on-stream under oxidizing conditions. Under reducing conditions, the release of

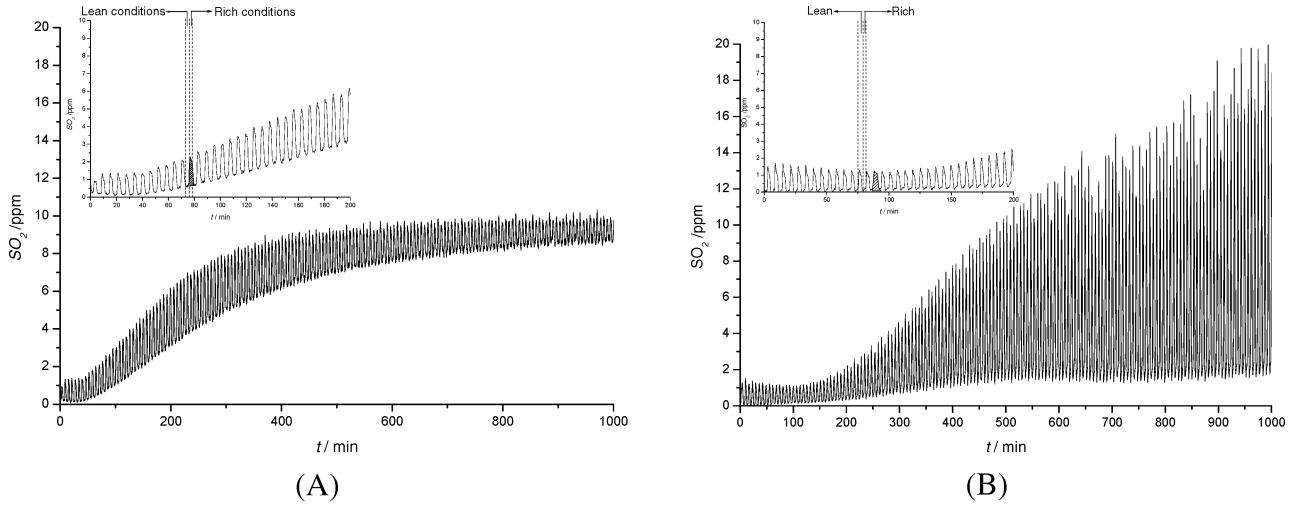

Figure 1. Plug flow experiments at lean−rich cycling conditions with gas compositions described in Table 1 on Ba/CuO−Al_2O_3 (A) and Ba/CuO−Al_2O_3 Pt (B) for 144 s for rich conditions at 523 K (inset = t = 200 min).

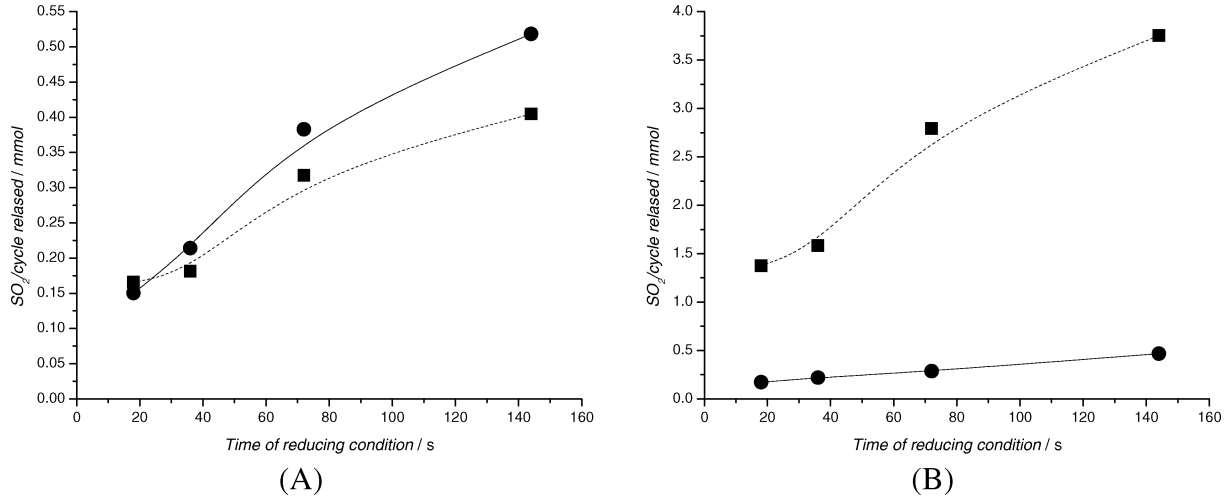

Figure 2. SO_2 released per cycle in the breakthrough experiments in dependence of rich cycling time on Ba/CuO−Al_2O_3 (full circles) and Ba/CuO−Al_2O_3 Pt (squares) (t = 0−50 min (A) and t = 950 − 1000 min (B)).

SO_2 was observed; however, it was diminished as compared to dry conditions. On the Pt containing material, this effect was only observed at a low time-on-stream. Varying the time for reduction (experiments not shown here), a similar behavior as compared to dry conditions was observed, indicating that an extended time under reducing conditions leads to enhanced SO_2 release. Experiments carried out only under lean conditions (not shown here) in the presence of water showed a higher overall SO_2 uptake capacity as compared to dry conditions, indicating that H_2O promotes SO_x sorption. The presence of C_3H_6 and CO_2 did not affect the total SO_x storage capacity, while for NO_2, a minor increase of the total sorption capacity was observed.

Influence of Pt on the SO_2 Adsorption during Lean−Rich Cycling Conditions. The influence of Pt on the SO_x storage process was studied by in situ IR spectroscopy on the Ba/CuO−Al_2O_3 Pt material shown in Figure 4. Two well-defined bands at 1552 and 1447 cm^{-1}, assigned to barium carbonate, were initially observed. After exposure to SO_2, bands at 1251, 1162, and 1040 cm^{-1} were formed, which are assigned to bulk sulfate species on Ba/CuO−Al_2O_3. The formation of the surface sulfate species identified on the parent material was observed in a similar region from 1350−1290 cm^{-1} (marked with a rectangle). In general, the positions of the bands on the Pt containing materials are similar to those on the Pt free sample (see part one[12]).

To identify the spectral regions affected during the lean−rich cycling, the Moving Window 2-D Correlation Analysis was applied. The synchronous contour plots obtained for lean and lean−rich conditions are depicted in Figure 5. Under lean conditions (see Figure 5A), three well-defined auto peaks located on the diagonal at 1290, 1160, and 1005 cm^{-1} were found, which form a square with cross-peaks at the corresponding intersections with a positive sign, indicating that the corresponding bands are increasing during lean operation mode. The slight shift as compared to the real position in the 1-D spectra results from the restricted range of spectra as well as the small number of spectra used for the analysis, as already described by Czarnecki,[18] which the identification of the spectral region perturbed. The negative peaks at the intersections of 1005, 1160, and 1290 cm^{-1} with 1430 cm^{-1} reveal that the corresponding species (carbonates) decrease during lean conditions. The spectral intensities at 1580 cm^{-1} (assigned to carbonate species) show a positive correlation with the attributed sulfate species at 1005, 1160, and 1290 cm^{-1}, indicating similar time-resolved behavior. This would suggest carbonate formation under lean conditions. However, as in this region additional nitrates also contribute to the spectrum, we speculate that this effect results from the interaction with NO_2. The result (a higher amount of NO_x adsorption) derived from the data analysis of the in situ NO_x experiments for the sample containing Pt support this result

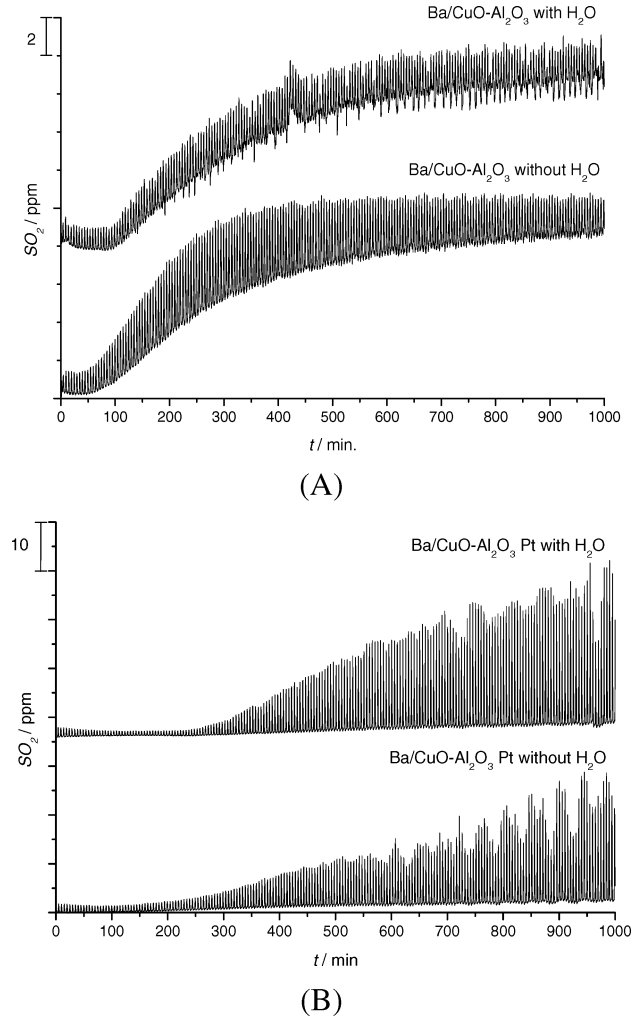

Figure 3. Plug flow experiments under lean−rich cycling conditions in the absence and in presence of 10% H_2O (upper line) on Ba/CuO−Al_2O_3 (A) and Ba/CuO−Al_2O_3 Pt (B) at $t = 72$ s for rich conditions.

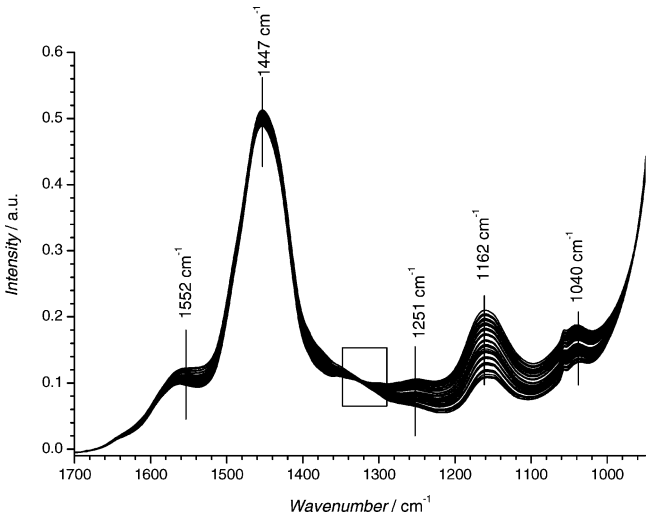

Figure 4. IR spectra of Ba/CuO−Al_2O_3 Pt recorded during lean (240 s)−rich (18 s) cycling at 523 K at the conditions described in Table 1 after 2 h lean conditions.

(not shown here). Figure 5B depicts the synchronous contour plot obtained for a set of spectra containing lean and rich conditions. It can be clearly seen that the intersections of 1150 and 1040 cm^{-1} with the carbonate species located at 1350 cm^{-1} are centered in a negative area (marked in gray), indicating that

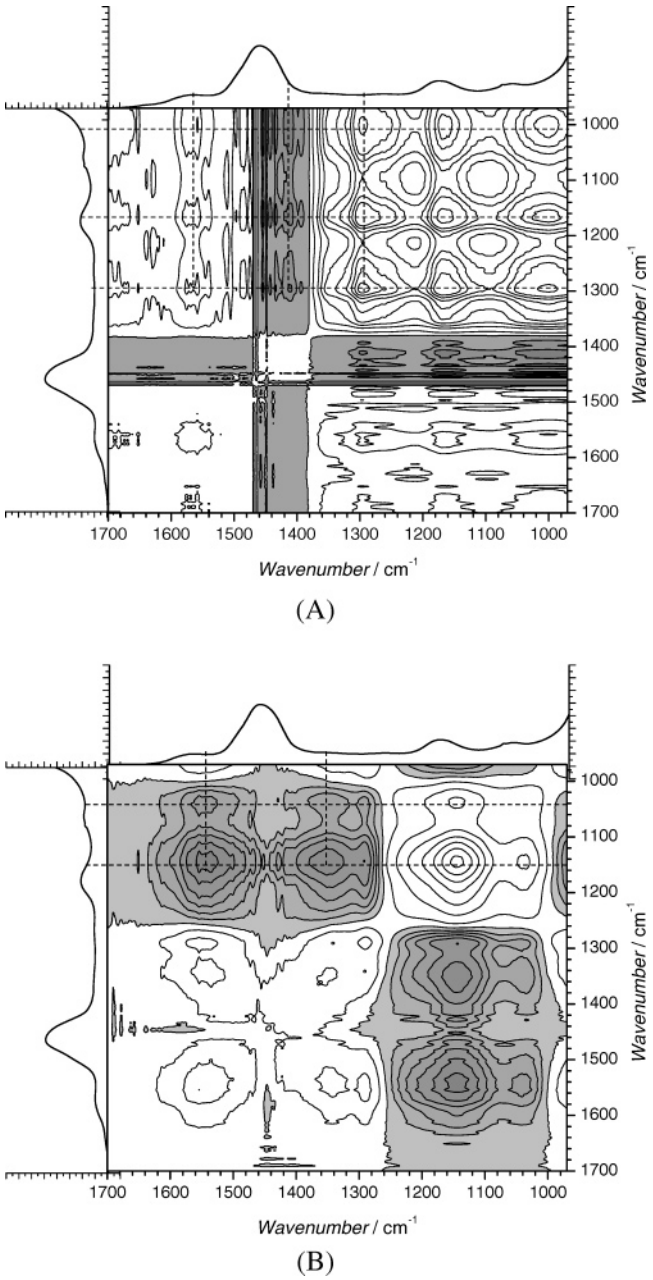

Figure 5. Synchronous plots calculated with the moving window concept: (A) calculated from spectra entirely recorded under lean conditions and (B) calculated from spectra recorded under lean and rich conditions on Ba/CuO−Al_2O_3 Pt.

the intensity of the peak located at 1350 cm^{-1} is decreasing also during rich operation mode, which might result from a decomposition of the nitrate species. A similar pattern is observed for the region around 1560 cm^{-1}, which suggests a diminishing of the probable NO_x species while bulk sulfates are formed under reducing conditions.

After the identification of the perturbed spectral regions, the pure components were determined applying MCR-ALS to the dataset using the diagonals of the 2-D Sample−Sample Correlation matrices as an initial concentration matrix (not shown here, see part one). The diagonal of a 2-D Sample−Sample Correlation Analysis represents the variations in the spectral intensities from the selected dataset and is therefore essential for the determination of physically meaningful information in the MCR-ALS. The 2-D Sample−Sample Correlation analysis allowing direct tracking of the concentration profiles in the spectral range included is a significant improvement as com-

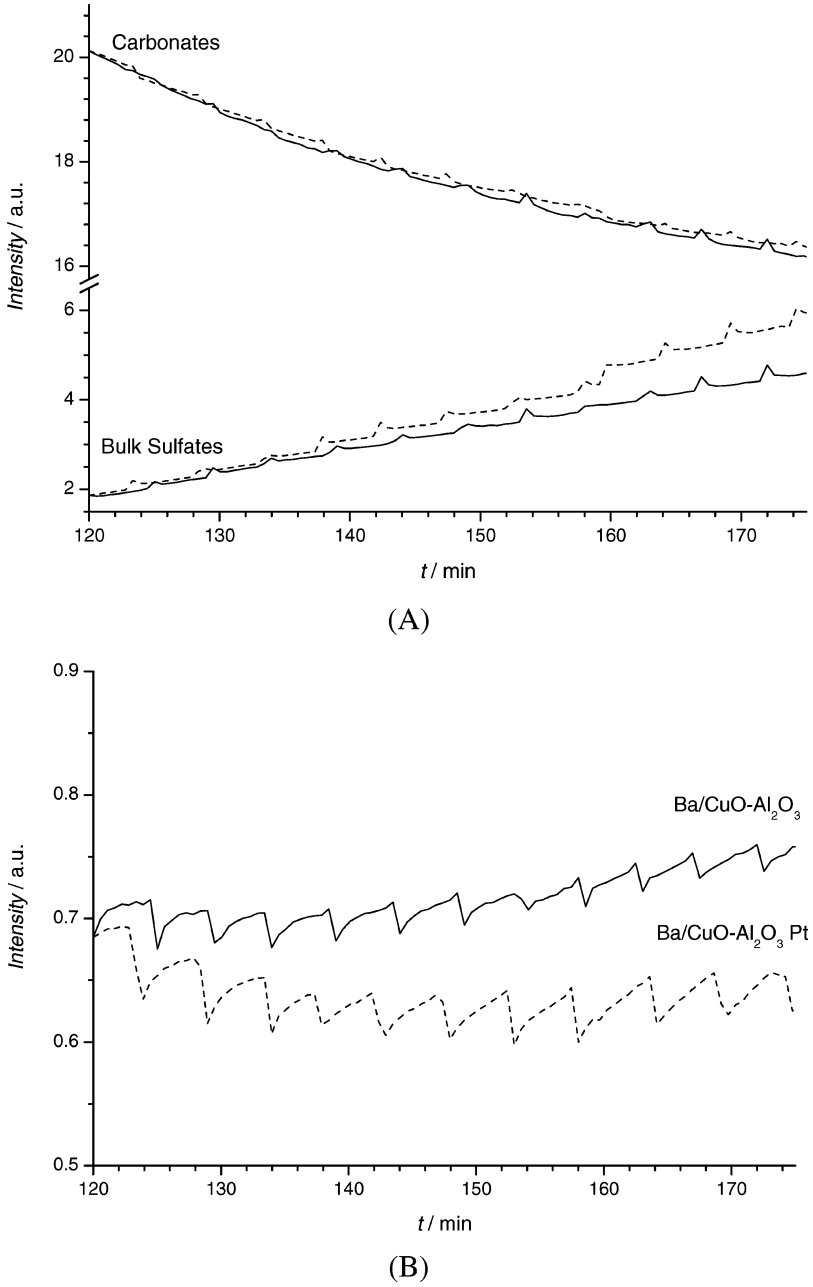

Figure 6. Diagonal traces obtained from the 2-D Sample−Sample Correlation Analysis of the carbonate and sulfate species (A) and surface species (B). (Ba/CuO−Al_2O_3 bold line and Ba/CuO−Al_2O_3 Pt dotted line). Note that all graphs were adjusted to the same intensity at the first point.

pared to the analysis of single time-resolved spectra. Similar carbonate and sulfate species were identified as compared to the Pt free sample. To compare the time-resolved behavior of the spectral intensities, the 2-D Sample−Sample Correlation Analysis was carried out on the same spectral regions as on the Pt free sample.[12] The results are shown in Figure 6. The dashed lines represent the sample containing Pt and the solid lines the Pt free sample. Only the traces along the diagonal of the 2-D Sample−Sample Correlation Analysis are plotted here (note that an offset was applied to all spectral intensities to simplify the comparison).

The spectral intensities attributed to the carbonate species (Figure 5A, decreasing lines) and bulk sulfate species (Figure 5A, increasing lines) for both materials show a similar trend with a slightly higher slope for the bulk sulfate species on the Pt containing material, indicating a higher amount of sulfates present on the material. It is important to note that the intensity of the spikes observed while switching to the rich operation mode are less pronounced for the Pt containing sample.

The pattern obtained for the transient sulfate species (see Figure 5B) shows that on both materials, the reduction of the surface species during the rich operation mode leads to a saw-tooth pattern. Moreover, for the Pt free sample, the increasing intensity indicates that the concentration of surface sulfate species increases over time, while for the Pt containing sample, the slight decrease indicates a smaller amount of surface species being present. However, the intensity of the oscillations during the lean−rich cycling shows that the amplitude of the oscillations is approximately twice as high for the Pt containing sample as compared to the Pt free sample, which strongly suggests that Pt facilitates the reduction of the transient sulfate species.

SO_2 Adsorption in the Presence of H_2O during Lean−Rich Cycling Conditions. The presence of H_2O diminished the SO_2 release under rich conditions as shown by the plug flow

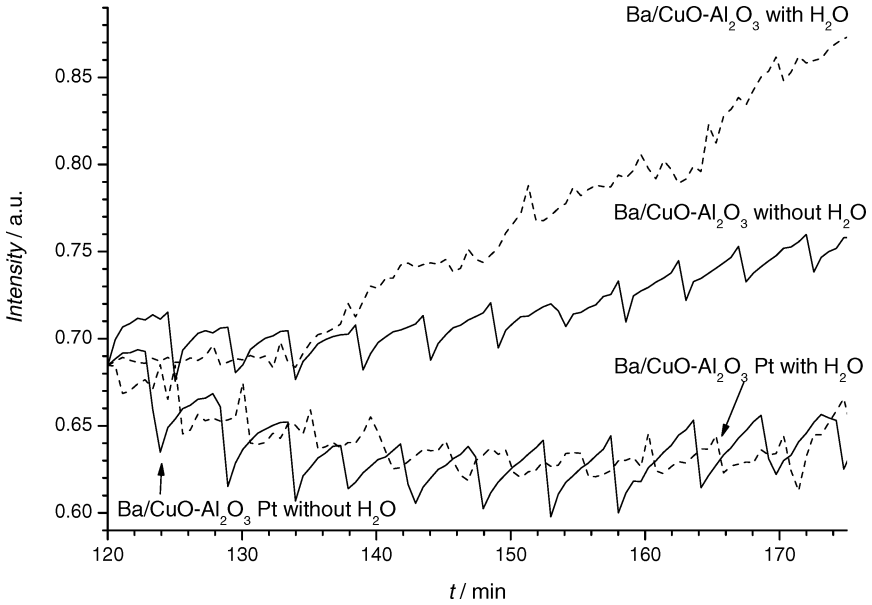

Figure 7. Diagonal traces of the 2-D Sample−Sample Correlation Analysis (1350−1290 cm^{-1}). The dashed lines represent wet conditions and the solid lines dry conditions.

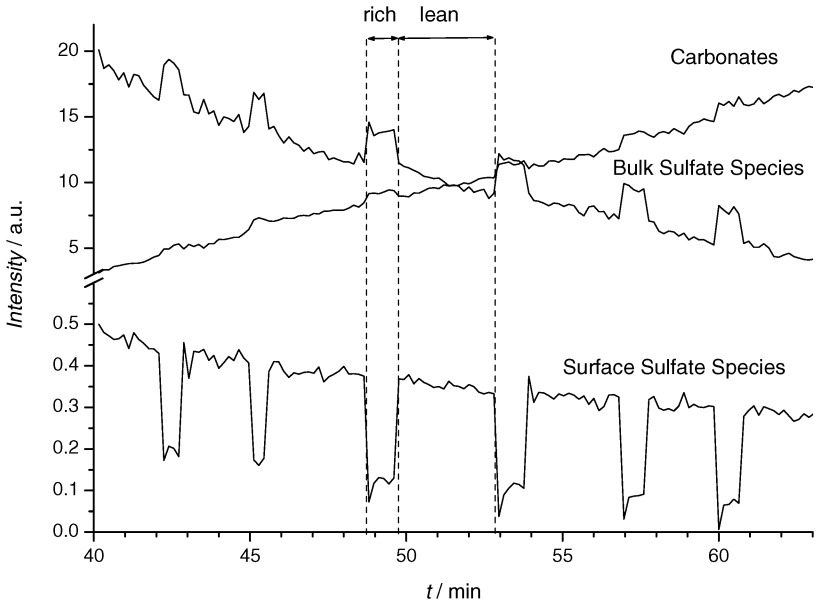

Figure 8. Diagonal lines obtained from the 2-D Sample−Sample Correlation Analysis of the surface species and carbonate and sulfate species on the Ba/CuO−Al_2O_3 with $t = 240$ s (lean) and $t = 72$ s (rich) with the conditions described in Table 1 at 523 K.

experiments (see Figure 3). On all samples investigated, a small peak at 1641 cm^{-1} and a broad peak around 3300 cm^{-1} were observed (graphs not shown), which are assigned to physisorbed water.[19] During in situ IR experiments in the presence of 10% water, similar bands for the bulk sulfate species and the carbonate species were observed. However, the intensity of the bulk sulfate species is higher, and the intensity of the bands assigned carbonates is decreasing faster as compared to dry conditions (not shown here). The comparison of the concentration profiles obtained by 2-D Sample−Sample Correlation Analysis over the region from 1350−1290 cm^{-1} for the Pt containing and Pt free material in the absence and presence of water is shown in Figure 7. The strong effect of water is clearly observed. The saw-tooth pattern of the transient sulfate species obtained under dry conditions is almost completely removed (see Figure 7, solid and dashed line), which indicates only a small reduction of this species in the presence of water on the Ba/CuO−Al_2O_3 Pt material. However, the overall intensity of the band under lean conditions is not strongly affected by the presence of water on the Pt containing sample, indicating a similar concentration of the surface species present. On the Ba/CuO−Al_2O_3 material, the saw-tooth pattern completely disappeared in the presence of water (dotted line), and the increasing intensity of the surface sulfate species suggests an accumulation of this species. It is important to note that under dry conditions the oscillatory behavior is approximately 2 times higher in the presence of Pt as compared to the Pt free sample.

Influence of Rich Condition Time on the SO_2 Adsorption during Lean−Rich Cycling Conditions. The influence of the time under rich conditions in the absence of water was investigated to determine the increasing SO_2 release observed under plug flow conditions (see Figures 1 and 2). The graphs depicted in Figure 8 represent the diagonal traces from the 2-D Sample−Sample Correlation Analysis performed on a dataset obtained from the Pt free sample (240 s lean/72 s rich). For the carbonate species, a decreasing intensity was observed overlaid

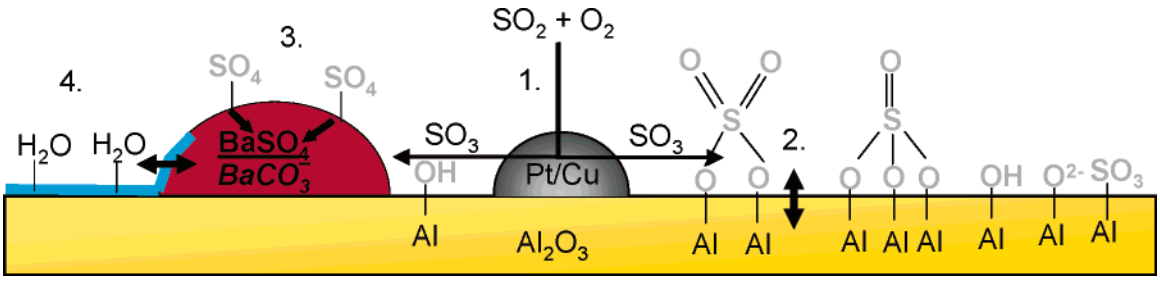

Figure 9. Simplified reaction network for the SO_x storage process on a second generation sulfur trapping material.

by a characteristic step-like pattern during switching to rich conditions. The spike pattern observed at shorter reduction time is transformed into a step-like pattern, possibly due to the prolonged exposure to a reducing atmosphere. The overall concentration of bulk sulfate species is increasing, also showing sharp step-like signals during the changes in gas composition. In comparison to the shorter cycling time, two clearly defined and equilibrated surface concentrations were established

Discussion

The physicochemical characterization of the sol−gel derived $CuO-Al_2O_3$ based material impregnated with Ba^{2+} and Pt shows that $BaCO_3$ particles are present on an amorphous $CuO-Al_2O_3$ support. The SO_2 uptake experiments carried out under cycling conditions confirmed the release of SO_2 under rich conditions, which is far more pronounced for the Pt containing material. This strongly suggests that Pt accelerates the reducibility of sulfur species.

In situ XANES at the S K-edge on that same material indicated that the sulfite species formed under fuel lean conditions is easily decomposed in the presence of Pt under fuel rich conditions and thus could lead to the formation of SO_2.[11] However, the sulfate species was not distinguished in detail due to the limitations of the XANES to differentiate between sulfur species of the same oxidation state. In situ IR spectra under typical exhaust gas compositions at 523 K reveal the formation of various sulfate species present on the surface and in the bulk during the lean−rich cycling conditions.

However, a wide variety of NO_x species is formed in the presence of NO_2. These surface groups are also reduced under rich conditions, leading to variations of intensity in the specific regions of the IR spectra. Consequently, the simultaneous presence of NO_x species results in a spike pattern on the 2-D sample−sample correlation analysis, masking all experiments.

General Aspects of the SO_x Storage Process. Figure 9 summarizes the results obtained in a simplified reaction network. Generally, in the presence of O_2, SO_2 is oxidized to SO_3 (1) and afterward trapped on the storage sites (2 and 3). Accessible Ba^{2+} sites are more stable as compared to Al^{3+} sites.[20,21] The lean−rich cycling experiments under plug flow conditions showed clearly that Cu is a sufficient oxidation component for the first step. Its lower reduction potential even leads to less SO_2 under rich conditions as compared to noble metals such as Pt.[22] The formation of the surface sulfate (2) as well as the bulk-like sulfate species (3) could be confirmed by the results obtained from the MCR-ALS. The removal of the surface sulfate (2) was also observed when applying lean−rich conditions, indicating a labile bonding. However, the presence of surface sulfates is needed to transfer sulfate into the bulk. Thus, a relatively large steady-state concentration of the surface sulfate enhances the uptake into bulk, and consequently, longer reduction times should be avoided.

Influence of Pt on the SO_2 Storage Process. 2-D Sample−Sample Correlation Analysis shows higher amplitudes of the changes in the surface concentrations of the transient species on the Pt containing materials, when cycling between rich and lean reaction conditions. In addition, the overall intensity of sulfates observed in the IR spectra is higher, indicating a higher amount of sulfates formed on the material. This strongly suggests that the formation as well as the reduction of this species on the surface of the SO_x trap is strongly affected by the presence of Pt.

The reaction is accelerated in the presence of Pt leading to higher SO_2 concentrations in the exhaust gas during the time-on-stream experiments because of the higher concentrations of sulfates accumulated over time.[23] Note that the intensities on the comparison of the spectra were set to the same start point.

This result is supported by the lower intensity in the spikes observed for this material on the concentration profile of the NO_x species, indicating a more pronounced reduction/oxidation behavior of Pt regarding NO/NO_2, which was already described for $DeNO_x$ catalysis.[3,24−26] This lets us conclude that the presence of Pt enhances the formation of the sulfates as well as the reduction of the nitrates. The higher concentrations of SO_2 released under dynamic conditions is therefore attributed to the reduction of more surface sulfates under fuel rich conditions. It is interesting to note that Pieplu et al.[27] suggested a kinetic model for the sulfation of pure Al_2O_3 involving the formation of additional free Al sites during the sulfate reduction. The accelerating effect of Pt could lead, therefore, to a higher concentration of free Al sites, resulting in a higher total concentration of surface sulfate species formed in the next cycle, which are in turn reduced under fuel rich conditions. For a complete protection and a long-term durability of the NSR catalyst, it seems to be sufficient to have a Pt free sample resulting in lower SO_2 concentrations released under rich conditions.[7,9]

Influence of Water on the SO_x Storage. Water enhances the total SO_2 storage capacity and lowers the SO_2 release under rich conditions. In situ IR spectroscopy shows that in the presence of water, only bulk and surface carbonates were present. For the Pt containing sample, the oscillations in the concentration of surface species during periodic lean−rich cycling are less pronounced in the presence of water as compared to the absence of water. This indicates that the lower concentration of SO_2 released in the presence of water could result from a lower concentration of a surface sulfate species reduced under rich conditions. This is tentatively attributed to a faster transport into the bulk phase accelerated by the formation of sulfuric acid. Therefore, we propose that the surface sulfate species identified on Al_2O_3 is mainly affected by the presence of water leading to a more stable conformation.[23] The higher total SO_2 sorption capacity could result from the formation of sulfuric acid, for which at 523 K thermodynamic limitations do not exist. This leads to a faster transport of surface

sulfates into the bulk phase of the material, similar to what has been observed with other oxide based materials.[28] This is supported by in situ XANES at the S K-edge, pointing out that in the presence of 10% water, a smaller fraction of sulfites is present on both samples as compared to dry conditions.[11] It shows also that the oxidation is facilitated by the presence of water.

The rate of carbonate decomposition is also reported to be higher in the presence of water, which is speculated to lead to a higher concentration of Ba^{2+} sites able to form bulk species. This reaction lowers in turn the coverage of the surface due to a faster bulk transport of sulfates.[29,30] This is in perfect agreement with the findings of higher bulk sulfate fractions detected by means of IR spectroscopy.

Influence of the Duration of Fuel Rich Conditions. Besides the presence of water, the release of SO_2 is mainly influenced by the time period under reducing conditions. The results show that the general trend of the concentration variations of the bulk carbonate and sulfate species is enforced at longer cycles under reducing reaction conditions. However, higher reduction times also lead to an unfavorable increase in fuel consumption, diminishing the advantage of a lean burning engine. A strong influence on the surface sulfate species was detected by increasing the reduction time to 72 s. The spikes observed for the spectral intensities attributed to carbonates and bulk sulfates are transformed into step shaped features due to the enlarged reduction period. Nevertheless, the general trend (i.e., the formation under oxidizing conditions and the removal after switching back to fuel rich mode of 240 s) is still observed. The results obtained for the surface species being located in the region from 1350 to 1290 cm^{-1} are also in perfect agreement with the saw-tooth pattern found for these spectral intensities. It is observed that the amount to which the surface species is reduced is far more pronounced than for a reducing period of 18 s.

Furthermore, the maximum storage capacity obtained under lean conditions was not reached. It should be taken into account that a low SO_2 concentration in the gas phase (10 ppm) additionally favors the desorption under rich conditions. As shown previously, the surface sulfate is the one mainly affected, leading to a more mobile sulfate species,[31−33] and the continuous formation and reduction makes it possible to migrate readily over the sorbent surface. In this context, it is interesting to mention that the quantification of the sulfur content on a monolith coated with these materials (not shown here) clearly showed a higher sulfur concentration in the end of the monolith. The removal of the species from the surface and the lower averaged surface concentration consequently lead to a lower concentration of bulk sulfate formation, resulting in underutilizing the theoretical storage amount.

It is speculated that this effect is the reason for the high stability of the NSR catalyst at low sulfur contents. The formation of a higher amount of stable bulk sulfate (Figure 9−, step 3) in the presence of water was shown by IR. Therefore, the presence of water (Figure 9, step− 4) seems to be essential for a high storage capacity. This is attributed to faster carbonate decomposition and the formation of sulfuric acid leading to a faster bulk transport.

Conclusion

The multiple and combined application of a variety of physicochemical techniques allows the identification of three spectral regimes showing characteristic patterns: (i) carbonates decreasing in concentration with time, (ii) bulk sulfates generally increasing with time, and (iii) surface sulfate species that follow the periodic changes in the gas-phase composition, thus having a characteristic saw-tooth pattern.

The reduction of the transient surface sulfate species contributes mainly to the SO_2 release observed under dynamic flow conditions. Pt as a noble metal facilitates the formation and reduction of this species, leading to a higher concentration of SO_2 released under rich conditions. From this point of view, noble metal free storage materials are preferred.

The ubiquitously present water reduces the SO_2 release during fuel rich operation mode. In the presence of water, the reduction of the surface species is suppressed, resulting in a faster transport into the bulk. However, increasing the reduction time mainly leads to a higher concentration of surface sulfates that are reduced and contributes to a higher SO_2 release during the regeneration cycle.

In contrast, the type and concentration of the bulk type sulfates does not lead to variations in the release or uptake kinetics during the periodic cycles under oxidizing and reducing reaction conditions. This exemplifies that at large, the sensitivity toward the formation of surface sulfates is responsible for the varying degree of sulfur release during the fuel lean/fuel rich cycles. Thus, the key parameter for SO_2 storage materials is to ensure a high capacity of strong adsorption sites on the surface.

Acknowledgment. This work was supported by the European Union in the framework of Project G3RD-CT2002 00793.

References and Notes

(1) Epling, W. S.; Campbell, L. E.; Yezerets, A.; Currier, N. W.; Parks, J. E. *Catal. Rev.—Sci. Eng.* **2004**, *46*, 163.
(2) Sedlmair, C.; Seshan, K.; Jentys, A.; Lercher, J. A. *Res. Chem. Intermed.* **2003**, *29*, 257.
(3) Sedlmair, C.; Seshan, K.; Jentys, A.; Lercher, J. A. *J. Catal.* **2003**, *214*, 308.
(4) Dathe, H.; Peringer, E.; Roberts, V.; Jentys, A.; Lercher, J. A. *C. R. Chim.* **2005**, *8*, 753.
(5) Li, L. Y.; King, D. L. *Ind. Eng. Chem. Res.* **2005**, *44*, 168.
(6) Dathe, H.; Jentys, A.; Haider, P.; Schreier, H.; Fricke, R., Lercher, J. A. *Phys. Chem. Chem. Phys.* **2006**, *8*, 1601.
(7) Limousy, L.; Mahzoul, H.; Brilhac, J. F.; Gilot, P.; Garin, F.; Maire, G. *Appl. Catal., B* **2003**, *42*, 237.
(8) Bailey, O. H.; Dou, D.; Molinier, M. *Soc. Automot. Eng., [Spec. Publ.] SP* **2000**, *1533*, 257.
(9) Fang, H. L.; Wang, J. C.; Yu, R. C.; Wan, C. Z.; Howden, K. *Soc. Automot. Eng., [Spec. Publ.] SP* **2003**, *1801*, 185.
(10) Limousy, L.; Mahzoul, H.; Brilhac, J. F.; Garin, E.; Maire, G.; Gilot, P. *Appl. Catal., B* **2003**, *45*, 169.
(11) Dathe, H.; Jentys, A.; Lercher, J. A. *J. Phys. Chem. B* **2005**, *109*, 21842.
(12) Dathe, H.; Haider, P.; Jentys, A.; Lercher, J. A. *J. Phys. Chem. B* **2006**, *110*, 10729.
(13) Noda, I.; Dowrey, A. E.; Marcott, C.; Story, G. M.; Ozaki, Y. *Appl. Spectrosc.* **2000**, *54*, 236.
(14) Sasic, A. S.; Muszynski A.; Ozaki, Y. *J. Phys. Chem. A* **2000**, *104*, 6380.
(15) Malinowski, E. R. *Factor Analysis in Chemistry*, 3rd ed.; John Wiley & Sons, Ltd.: New York, 2002.
(16) Tauler, R.; de Juan, A. MATLAB program MCR-ALS, MATLAB program EFA; http:/www.ub.es/gesq/eq1_eng.htm (accessed 2/16/2006), 2003.
(17) Mazet, V.; Carteret, C.; Brie, D.; Idier, J.; Humbert, B. *Chemom. Intell. Lab. Syst.* **2005**, *76*, 121.
(18) Czarnecki, M. A. *Appl. Spectrosc.* **2000**, *54*, 986.
(19) *(19) Al-Hosney, H. A.; Grassian, V. H. Phys. Chem. Chem. Phys.* **2005**, *7*, 1266.
(20) Centi, G.; Passarini, N.; Perathoner, S.; Riva, A. *Ind. Eng. Chem. Res.* **1992**, *31*, 1947.
(21) Centi, G.; Passarini, N.; Perathoner, S.; Riva, A. *Ind. Eng. Chem. Res.* **1992**, *31*, 1956.
(22) Kent, S. A.; Katzer, J. R.; Manogue, W. H. *Ind. Eng. Chem. Fundam.* **1977**, *16*, 443.
(23) Summers, J. C. *Environ. Sci. Technol.* **1979**, *13*, 321.

(24) Amberntsson, A.; Fridell, E.; Skoglundh, M. *Appl. Catal., B* **2003**, *46*, 429.
(25) Fridell, E.; Skoglundh, M.; Westerberg, B.; Johansson, S.; Smedler, G. *J. Catal.* **1999**, *183*, 196.
(26) Su, Y.; Amiridis, M. D. *Catal. Today* **2004**, *96*, 31.
(27) Pieplu, A.; Saur, O.; Lavalley, J. C.; Pijolat, M.; Legendre, O. *J. Catal.* **1996**, *159*, 394.
(28) Dathe, H.; Jentys, A.; Lercher, J. A. *Phys. Chem. Chem. Phys.* **2005**, *7*, 1283.
(29) Terry, B. S.; McGurk, G. *Trans. Inst. Min. Metall., Sect. C* **1994**, *103*, 62.
(30) L'Vov, B. V. *Thermochim. Acta* **1997**, *303*, 161.
(31) Waqif, M.; Saur, O.; Lavalley, J. C.; Perathoner, S.; Centi, G. *J. Phys. Chem.* **1991**, *95*, 4051.
(32) Yoo, K. S.; Jeong, S. M.; Kim, S. D.; Park, S. B. *Ind. Eng. Chem. Res.* **1996**, *35*, 1543.
(33) Yoo, K. S.; Kim, S. D.; Park, S. B. *Ind. Eng. Chem. Res.* **1994**, *33*, 1786.